


Interface-Generated Spin Currents

V. P. Amin,^{1,2,*} J. Zemen,³ and M. D. Stiles²

¹Maryland NanoCenter, University of Maryland, College Park, Maryland 20742

²Center for Nanoscale Science and Technology, National Institute of Standards and Technology, Gaithersburg, Maryland 20899, USA

³Faculty of Electrical Engineering, Czech Technical University in Prague, Technick 2, Prague 166 27, Czech Republic

 (Received 12 March 2018; published 26 September 2018)

Transport calculations based on *ab initio* band structures reveal large interface-generated spin currents at Co/Pt, Co/Cu, and Pt/Cu interfaces. These spin currents are driven by in-plane electric fields but flow out of plane and can have similar strengths to spin currents generated by the spin Hall effect in bulk Pt. Each interface generates spin currents with polarization along $\hat{\mathbf{z}} \times \mathbf{E}$, where $\hat{\mathbf{z}}$ is the interface normal and \mathbf{E} denotes the electric field. The Co/Cu and Co/Pt interfaces additionally generate spin currents with polarization along $\hat{\mathbf{m}} \times (\hat{\mathbf{z}} \times \mathbf{E})$, where $\hat{\mathbf{m}}$ gives the magnetization direction of Co. The latter spin polarization is controlled by—but not aligned with—the magnetization, providing a novel mechanism for generating spin torques in magnetic trilayers.

DOI: 10.1103/PhysRevLett.121.136805

Introduction.—An important goal of spintronics research is to discover efficient methods of spin current generation. Although experiments continue to illuminate new routes towards this objective, there are few quantitative estimates of spin current generation in realistic material systems. Exceptions include calculations of the spin Hall effect [1–7], which converts a charge current into a transversely flowing spin current. First principles calculations of spin Hall conductivities have played a crucial role in corroborating experimental results. The vitality of other methods of spin current generation is similarly tied to the ability to make realistic quantitative predictions.

Recent work has shown that interfaces with spin-orbit coupling generate spin currents when driven by an electric field in the interface plane [8,9]. These interface-generated spin currents can flow out of the interface plane and exert spin torques on adjacent or nearby ferromagnet layers. Like the spin Hall effect, these interface-generated spin currents convert a charge current into a transversely flowing spin current. Because of the reduced symmetry of the interface, the interface-generated spin current flowing out of plane can be written as

$$\mathbf{j} = j_f \hat{\mathbf{s}} + j_p \hat{\mathbf{m}} \times \hat{\mathbf{s}} + j_m \hat{\mathbf{s}} \times (\hat{\mathbf{m}} \times \hat{\mathbf{s}}), \quad (1)$$

where the three-vector \mathbf{j} points along the spin polarization direction. For high symmetry interfaces, $\hat{\mathbf{s}} \equiv \hat{\mathbf{z}} \times \mathbf{E}$, where $\hat{\mathbf{z}}$ points out of plane. At nonmagnetic interfaces, j_p and j_m vanish. At ferromagnet-nonmagnet interfaces, j_m vanishes when $\hat{\mathbf{m}}$ points in plane or out of plane. Figure 1 summarizes interface-generated spin currents.

In this Letter, we report the strength and magnetization dependence of interface-generated spin currents using first principles transport calculations. We find that Co/Pt,

Co/Cu, and Pt/Cu interfaces generate spin currents with coefficients similar to spin Hall conductivities reported in Pt and are as large as $\approx 1500 \Omega^{-1} \text{cm}^{-1}$ [10]. The spin currents injected into ferromagnetic layers dephase and create spin-orbit torques. Here we focus on the spin currents injected into nonmagnetic layers, which can traverse that layer and create torques on a remote ferromagnetic layer. These spin currents enable field-free switching of perpendicularly magnetized layers in ferromagnetic trilayers [11], potentially important for the development of magnetic memories. Evidence of torques exerted by such spin currents has been observed in NiFe/Ti/CoFeB and CoFeB/Ti/CoFeB spin valves [11] and in more complex multilayered systems [12]. The strong spin current generation reported here not only provides a much needed quantitative estimate of spin current generation, it also paves the way for future theoretical and experimental investigations of spin current generation at

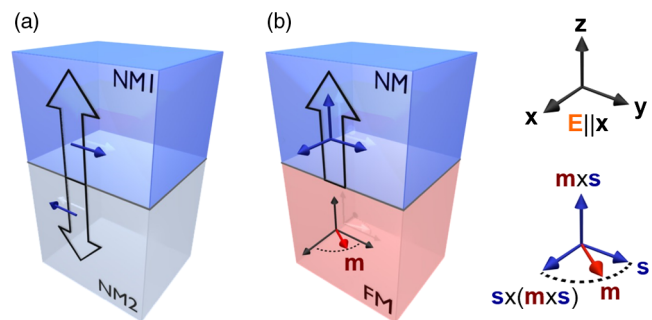


FIG. 1. Depiction of interface-generated spin currents at (a) nonmagnetic and (b) ferromagnet-nonmagnet interfaces driven by an electric field $\mathbf{E} \parallel \hat{\mathbf{x}}$. Block arrows show the spin flow direction ($\hat{\mathbf{z}}$) and blue arrows show the allowed spin polarization directions.

interfaces rather than in bulk materials, where the focus has centered on to date.

Spin-orbit filtering and precession.—A simple model [9,11] provides physical motivation for the important effects found in the first principles calculations of spin currents and torques. Based on this model, we call $j_{\ell}\hat{s}$ the spin-orbit filtering current and $j_{\rho}\hat{\mathbf{m}}\times\hat{s}$ the spin-orbit precession current (note that $j_m = 0$ in this model).

Spin-orbit filtering occurs because carriers with spins parallel and antiparallel to the interfacial spin-orbit field experience different scattering amplitudes [Fig. 2(a)] [13]. Thus, reflected and transmitted carriers are spin polarized even if incoming carriers are unpolarized. Spin-orbit filtering currents occur at nonmagnetic interfaces with spin-orbit coupling even if the bulk currents are unpolarized. Spin-orbit precession occurs when carriers precess about the interfacial spin-orbit field while scattering off the interface [Fig. 2(b)]. In the simplest models, carriers with opposite spins but the same incoming momentum precess identically while scattering, so the scattered spins remain opposite but have changed their overall orientation. Thus, the scattered carriers are polarized only if the incident carriers are polarized, so spin-orbit precession currents only occur if one layer is ferromagnetic.

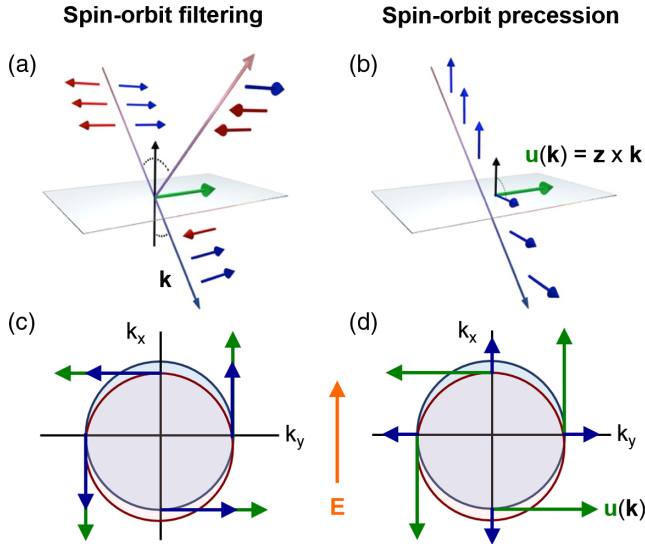


FIG. 2. (a) Spin-orbit filtering and (b) spin-orbit precession. Spin-orbit filtering occurs when the interfacial spin-orbit field $\mathbf{u}(\mathbf{k})$ (green arrow) filters reflected or transmitted electrons based on spin orientation. Spin-orbit precession occurs when electrons precess about the interfacial spin-orbit field during reflection and transmission. (c),(d) The transmitted in-plane spin density (blue arrows) for each incident momentum state for (c) spin-orbit filtering and (d) spin-orbit precession. The incident states shown belong to a constant k_z contour of the three-dimensional spherical Fermi surface. The green arrows represent the momentum-dependent spin-orbit field. Applying an electric field shifts the occupation of the incident electrons so that the transmitted electrons carry a net spin polarization.

The simple model to illustrate these processes assumes that carriers in both layers comprise free electron gases with identical, spin-independent, spherical Fermi surfaces. If one layer is ferromagnetic, we assume the imbalance of majority and minority carriers only arises in nonequilibrium. The interfacial potential has the form

$$V(\mathbf{r}) = \frac{\hbar^2 k_F}{m} \delta(z) [u_0 + u_R \sigma \cdot (\hat{\mathbf{k}} \times \hat{\mathbf{z}})], \quad (2)$$

where u_0 is a spin-independent barrier, u_R is the scaled Rashba parameter, k_F is the Fermi momentum, and $\hat{\mathbf{k}}$ is a unit vector pointing along the incident momentum. Electrons scattering from the potential in Eq. (2) have the transmission amplitudes

$$t^\pm(\mathbf{k}) = \frac{ik_z/k_F}{ik_z/k_F - [u_0 \pm u_{\text{eff}}(\mathbf{k})]}, \quad (3)$$

where the $+$ ($-$) label spins parallel (antiparallel) to the spin-orbit field defined by $\mathbf{u}(\mathbf{k}) = u_{\text{eff}}(\mathbf{k})\hat{\mathbf{u}}(\mathbf{k}) = u_R\hat{\mathbf{k}} \times \hat{\mathbf{z}}$.

To compute spin currents carried by an ensemble of electrons driven by an in-plane electric field \mathbf{E} , we determine the nonequilibrium distribution function $g_{\uparrow/\downarrow}(\mathbf{k})$. Here \uparrow/\downarrow denote spins parallel/antiparallel to the magnetization. For simplicity, we assume that electrons incident on the interface obey the relaxation time approximation, i.e. $g_{\uparrow/\downarrow}(\mathbf{k}) \propto E\tau_{\uparrow/\downarrow}k_x$ for $\mathbf{E} = E\hat{\mathbf{x}}$. Here $\tau_{\uparrow/\downarrow}$ give the momentum relaxation times for each spin species.

While the incident electrons have no net out-of-plane flow, the reflected and transmitted electrons carry a spin current that flows out of plane. In the following, we group the incident electrons into an unpolarized distribution $g^c = (g^\uparrow + g^\downarrow)/2$ and a spin-polarized distribution $g^s = (g^\uparrow - g^\downarrow)/2$. The transmitted spin currents from the unpolarized incident electrons \mathbf{j}'_{ℓ} and from the spin-polarized incident electrons \mathbf{j}'_{ρ} are

$$\mathbf{j}'_{\ell} \propto E(\tau_{\uparrow} + \tau_{\downarrow}) \int_{\text{FS}} d\mathbf{k}_{\parallel} k_x [|t^+(\mathbf{k})|^2 - |t^-(\mathbf{k})|^2] \hat{\mathbf{u}}(\mathbf{k}), \quad (4)$$

$$\mathbf{j}'_{\rho} \propto E(\tau_{\uparrow} - \tau_{\downarrow}) \int_{\text{FS}} d\mathbf{k}_{\parallel} k_x \mathbb{T}(\mathbf{k}) \hat{\mathbf{m}}, \quad (5)$$

where the total transmitted spin current is $\mathbf{j}' = \mathbf{j}'_{\ell} + \mathbf{j}'_{\rho}$ [11]. Here \mathbf{k}_{\parallel} denotes the in-plane momentum and $\mathbb{T}(\mathbf{k})$ is a 3×3 matrix that depends on $t^\pm(\mathbf{k})$. Note that $\tau_{\uparrow/\downarrow}$ correspond to the layer containing the incident electrons. Similar expressions exist for the spin currents $\mathbf{j}'_{\ell/\rho}$ carried by the reflected electrons. Further details, such as the explicit form of $\mathbb{T}(\mathbf{k})$, can be found in [11]. The total spin current is the sum of the reflected and transmitted spin currents given by $\mathbf{j}_{\ell/\rho} = \mathbf{j}'_{\ell/\rho} + \mathbf{j}''_{\ell/\rho}$, where $\mathbf{j}_{\ell} \propto \hat{\mathbf{s}}$ and $\mathbf{j}_{\rho} \propto \hat{\mathbf{m}} \times \hat{\mathbf{s}}$. Figures 2(c) and 2(d) depict how the sum of

transmitted spins over the incident momentum states yield this result when $\hat{\mathbf{s}} = \hat{\mathbf{y}}$.

The spin currents \mathbf{j}_f and \mathbf{j}_p arise from the spin-orbit filtering and spin-orbit precession mechanisms introduced earlier. The spin-orbit filtering current \mathbf{j}_f captures incident electrons being filtered by the spin-orbit field $\hat{\mathbf{u}}(\mathbf{k})$ during transmission. This filtering occurs if $|t^+(\mathbf{k})| \neq |t^-(\mathbf{k})|$, so that spins aligned with $\hat{\mathbf{u}}(\mathbf{k})$ have higher transmission probability than antialigned spins. The spin-orbit precession current \mathbf{j}_p captures incident spins oriented along $\hat{\mathbf{m}}$ being rotated by the spin-orbit field during transmission. This can be seen by showing that the matrix $\mathbb{T}(\mathbf{k})$ in Eq. (5) rotates $\hat{\mathbf{m}}$ about $\hat{\mathbf{u}}(\mathbf{k})$ [11].

In this model, the reflected and transmitted electrons only carry spin-orbit filtering and spin-orbit precession currents, so the coefficient j_m in Eq. (1) vanishes. Furthermore, the coefficients j_f and j_p are magnetization independent. However, adding an interfacial exchange interaction to Eq. (2) and obtaining the resulting interface-generated spin currents numerically [8,9] shows that j_f and j_p vary with magnetization and j_m only vanishes when $\hat{\mathbf{m}}$ points in plane or out of plane. This greater generality arises because the effective field u_{eff} is magnetization dependent in the presence of an interfacial exchange interaction. The transport calculations presented below demonstrate that the spin currents at Co/Cu, Co/Pt, and Pt/Cu interfaces exhibit this more general magnetization dependence.

Spin torques.—Spin currents that flow into ferromagnetic layers exert dampinglike spin transfer torques of the form $\tau \propto \hat{\mathbf{m}} \times (\hat{\mathbf{m}} \times \hat{\mathbf{p}})$, where $\hat{\mathbf{p}}$ equals the spin polarization direction of the spin current [14–18]. Since spin-orbit filtering currents and spin Hall currents have a fixed spin polarization $\hat{\mathbf{p}} = \hat{\mathbf{s}} = \hat{\mathbf{z}} \times \mathbf{E}$, both spin currents exert torques given by $\hat{\mathbf{m}} \times (\hat{\mathbf{m}} \times \hat{\mathbf{s}})$. Spin-orbit precession currents have a magnetization-dependent spin polarization given by $\hat{\mathbf{p}} = \hat{\mathbf{m}} \times \hat{\mathbf{s}}$. At a ferromagnet-nonmagnet interface, spin-orbit precession currents exert spin torques on the ferromagnetic layer of the form $\hat{\mathbf{m}} \times [\hat{\mathbf{m}} \times (\hat{\mathbf{m}} \times \hat{\mathbf{s}})] = \hat{\mathbf{m}} \times (-\hat{\mathbf{s}})$. Such torques can be thought of as inciting magnetization precession about $-\hat{\mathbf{s}}$. In general, we may classify spin torques as *dampinglike* [$\tau_{\text{DL}} \propto \hat{\mathbf{m}} \times (\hat{\mathbf{m}} \times \hat{\mathbf{s}})$] or *fieldlike* ($\tau_{\text{FL}} \propto \hat{\mathbf{m}} \times \hat{\mathbf{s}}$).

In trilayers consisting of a nonmagnetic spacer sandwiched between two ferromagnetic layers, the interface-generated spin currents injected into the nonmagnet can traverse that layer and exert torques on a subsequent magnetic layer, thereby coupling the magnetizations of the ferromagnetic layers. For instance, the interface between the bottom ferromagnetic layer and the nonmagnetic spacer emits a spin current that traverses the spacer layer and exerts a spin torque on the top ferromagnetic layer. This spin torque has the form $\hat{\mathbf{m}}_t \times [\hat{\mathbf{m}}_t \times (\hat{\mathbf{m}}_b \times \hat{\mathbf{s}})]$, where $\hat{\mathbf{m}}_{t(b)}$ describes the magnetization of the top (bottom) ferromagnetic layer. For the case of a fixed bottom layer with $\hat{\mathbf{m}}_b = \hat{\mathbf{x}}$, a free top

layer with $\hat{\mathbf{m}}_t = \hat{\mathbf{z}}$, and an electric field $\mathbf{E} \parallel \hat{\mathbf{x}}$, the spin-orbit precession current emitted from the bottom interface has polarization along $\hat{\mathbf{z}}$. Thus, spin-orbit precession currents can damp the magnetization towards the \mathbf{z} axis and therefore assist in switching perpendicularly magnetized ferromagnetic layers [11].

Interface-generated spin currents at Co/Cu, Co/Pt, and Pt/Cu interfaces.—First principles calculations show that interfaces significantly alter spin currents generated in bulk layers through spin memory loss [19,20] or by modifying the spin Hall angle [21]. We now demonstrate the converse in realistic systems: interfaces generate spin currents that will traverse neighboring bulk layers. To do so, we study both bulk materials (or infinite crystals) and bilayers (where each layer is a semi-infinite crystalline slab). The materials are composed of either Co, Cu, or Pt atoms. We use a tight-binding model fitted to first principles calculations to simulate the material systems [22,23] and Green's functions techniques to obtain the electronic wave functions, spin currents, and spin torques in the sample [24,25] [26].

To introduce an in-plane electric field (using the relaxation time approximation), we assume the nonequilibrium occupation of incoming states is proportional to $E\tau_\sigma^M v_{x,m\sigma}^M(\mathbf{k})$. Here, m gives the spin-independent band number, $\sigma \in [\uparrow/\downarrow]$ denotes the spin state, and $M \in [\text{Co}, \text{Cu}, \text{Pt}]$. The quantity τ_σ^M denotes the momentum relaxation time and $v_{x,m\sigma}^M(\mathbf{k})$ gives the x velocity (determined by the electronic structure). The momentum relaxation times are the only free parameters in this theory, and are chosen to reproduce the desired bulk conductivity and polarization in each layer. We do not compute the perturbation to the wave functions caused by the electric field or include the impurity scattering potentials that drive side-jump or skew scattering. Thus, our results exclude the spin Hall and anomalous Hall effects in all materials. However, spin-orbit coupling modifies the bulk Co eigenmodes in a magnetization-dependent way, thus capturing the anisotropic magnetoresistance or planar Hall effect [27–34].

Bulk currents arising from the planar Hall effect in Co complicate the analysis of interface-generated spin currents. Therefore we first discuss charge and spin currents in bulk materials with flow transverse to the electric field. As expected in the absence of the spin Hall and anomalous Hall effects, bulk Pt and Cu do not generate any transversely flowing charge or spin currents. However, bulk Co generates a transversely flowing charge current with a magnetization dependence consistent with the planar Hall effect. This charge current is accompanied by transversely flowing spin currents polarized along $\hat{\mathbf{m}}$ and $\hat{\mathbf{m}} \times \hat{\mathbf{s}}$. Figure 3(a) shows the magnetization dependence of these bulk spin currents. The former spin current is expected in ferromagnets while the latter is allowed by symmetry but not typically considered. Although the spin polarization of the latter spin current is misaligned with the magnetization, we find it exerts no spin torques and is continuous across

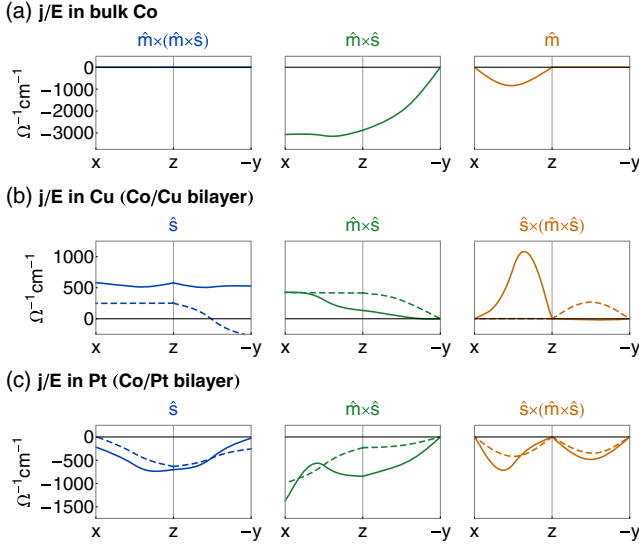


FIG. 3. Magnetization dependence of spin currents (\mathbf{j}) flowing out of plane ($\hat{\mathbf{z}}$) generated by an in-plane electric field ($\mathbf{E} \parallel \hat{\mathbf{x}}$). The magnetization is swept along the x/z plane followed by the z/y plane. (a) Bulk spin currents in Co, whose origin is closely related to the planar Hall effect. (b),(c) Spin currents in Cu and Pt layers (averaged over 14 monolayers) within the Co/Cu and Co/Pt bilayers. The solid curves give the total spin currents while the dashed curves give purely interface-generated spin currents (obtained by removing spin-orbit coupling from the Co layers).

each monolayer. All bulk-generated spin currents (flowing transverse to the electric field) vanish in the absence of spin-orbit coupling.

Next, we discuss the spin currents in bilayers that are driven by an in-plane electric field but flow out of plane. In accordance with the toy model described above, the Pt/Cu bilayer (not shown) only generates spin currents polarized along $\hat{\mathbf{s}}$ while the Co/Cu and Co/Pt bilayers generate spin currents polarized along $\hat{\mathbf{s}}$, $\hat{\mathbf{m}} \times \hat{\mathbf{s}}$, and $\hat{\mathbf{s}} \times (\hat{\mathbf{m}} \times \hat{\mathbf{s}})$. However, bulk spin current generation in the Co layers also contribute to these spin currents (discussed above). To isolate the interface-generated spin currents, we artificially remove spin-orbit coupling in the Co layers. The results are shown by the dashed curves in Figs. 3(b) and 3(c) and Fig. 4. Even with spin-orbit coupling eliminated in the Co layers, the interface-generated spin currents that escape into Cu and Pt are not significantly reduced.

In most devices utilizing spin-orbit torques, the spin Hall effect is thought to be intrinsic and not vary with the electron lifetimes. Thus, the ratio of the spin current flowing out of plane to the charge current flowing in plane is largest for low conductivity materials. Interface-generated spin currents scale with electron lifetimes (which are monotonically related to the conductivity) so the same ratio is largely independent of conductivity. These spin currents are therefore more likely to be important in high conductivity samples. The interface-generated spin currents in Co/Cu are comparable to measured Pt spin Hall conductivities

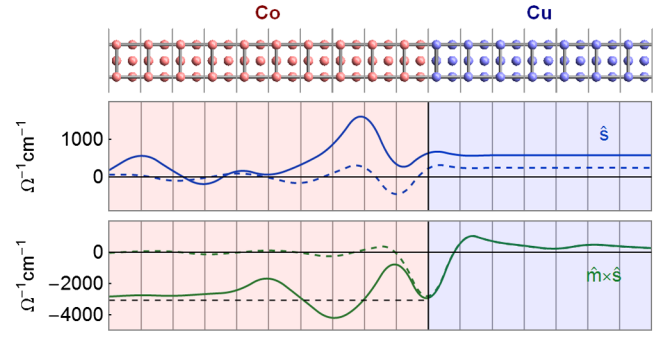


FIG. 4. Plot of the spin currents flowing out of plane ($\hat{\mathbf{z}}$) driven by an in-plane electric field ($\mathbf{E} \parallel \hat{\mathbf{x}}$) between each principal layer (two monolayers) in the Co/Cu bilayer (solid curves). Artificially removing spin-orbit coupling in Co eliminates the bulk contribution from that layer, giving purely interface-generated spin currents (dashed curves). The black horizontal dashed line gives the expected bulk contribution (taken from the bulk Co simulation).

ranging from $\approx 1300 \text{ } \Omega^{-1} \text{ cm}^{-1}$ – $1900 \text{ } \Omega^{-1} \text{ cm}^{-1}$ [35] and to theoretical estimates of $1300 \text{ } \Omega^{-1} \text{ cm}^{-1}$ [36] and $1600 \text{ } \Omega^{-1} \text{ cm}^{-1}$ [21]. The values generated by Co/Pt and Pt/Cu interfaces are even larger and fall within the range of the Pt spin Hall conductivities reproduced above, although larger estimates of $\approx 3000 \text{ } \Omega^{-1} \text{ cm}^{-1}$ have been obtained [37,38]. For Co/Pt bilayers, this suggests that strong competition might exist between the spin Hall effect and interface-generated spin currents.

An important question is whether it is possible to distinguish, in either experiments [39–41] or calculations, between spin currents generated from competing mechanisms. In addition to those we consider, other mechanisms include the anisotropic magnetoresistance, the spin anomalous Hall effect [42], and spin swapping [43,44]. The standard experimental technique to distinguish bulk and interface effects is to measure thickness dependences, but in these systems too many properties of the system change as layer thicknesses are varied. Symmetry considerations can eliminate some possible explanations, as in Ref. [11] where the spin anomalous Hall effect [42] was eliminated. In calculations, competing effects are easier to distinguish because they can often be turned on and off. For example, in these calculations, we eliminate the contributions from the anisotropic magnetoresistance by turning off the spin-orbit coupling in the bulk of the ferromagnet. We also eliminate any contributions from the spin anomalous Hall effect or related effects by neglecting the underlying mechanisms, such as skew or side-jump scattering and anomalous velocities.

We have demonstrated that Co/Cu, Co/Pt, and Pt/Cu interfaces driven by an in-plane electric field generate spin currents that flow out of plane ($\hat{\mathbf{z}}$). All three interfaces generate spin currents polarized along $\hat{\mathbf{s}} = \hat{\mathbf{z}} \times \mathbf{E}$. For the magnetic bilayers, both the interface and the bulk ferromagnetic layer additionally generate spin currents polarized

along $\hat{\mathbf{m}} \times \hat{\mathbf{s}}$ and $\hat{\mathbf{s}} \times (\hat{\mathbf{m}} \times \hat{\mathbf{s}})$. These additional spin currents could enable field-free switching in magnetic trilayers where the free ferromagnetic layer has perpendicular magnetic anisotropy. This family of bulk- and interface-generated spin currents present a novel mechanism to generate spin torques in magnetic heterostructures.

The authors thank Kyung-Jin Lee, Byong-Guk Park, Xin Fan, and Paul Haney for useful conversations and Robert McMichael and Justin Shaw for critical readings of the manuscript. V. A. acknowledges support under the Cooperative Research Agreement between the University of Maryland and the National Institute of Standards and Technology Center for Nanoscale Science and Technology, Award No. 70NANB14H209, through the University of Maryland.

* vivek.amin@nist.gov

- [1] M. I. D'yakonov and V. I. Perel, *JETP Lett.* **13**, 467 (1971).
- [2] J. E. Hirsch, *Phys. Rev. Lett.* **83**, 1834 (1999).
- [3] S. Zhang, *Phys. Rev. Lett.* **85**, 393 (2000).
- [4] S. Murakami, N. Nagaosa, and S.-C. Zhang, *Science* **301**, 1348 (2003).
- [5] J. Sinova, D. Culcer, Q. Niu, N. A. Sinitsyn, T. Jungwirth, and A. H. MacDonald, *Phys. Rev. Lett.* **92**, 126603 (2004).
- [6] Y. K. Kato, R. C. Myers, A. C. Gossard, and D. D. Awschalom, *Science* **306**, 1910 (2004).
- [7] J. Wunderlich, B. Kaestner, J. Sinova, and T. Jungwirth, *Phys. Rev. Lett.* **94**, 047204 (2005).
- [8] V. P. Amin and M. D. Stiles, *Phys. Rev. B* **94**, 104419 (2016).
- [9] V. P. Amin and M. D. Stiles, *Phys. Rev. B* **94**, 104420 (2016).
- [10] We use units of conductivity for spin currents. A spin current in units of a flux of angular momentum may be converted to units of a charge current density by multiplying by a factor of $2e/\hbar$, then to a conductivity by dividing by the electric field.
- [11] S. C. Baek, V. P. Amin, Y. Oh, G. Go, S.-J. Lee, M. D. Stiles, B.-G. Park, and K.-J. Lee, *Nat. Mater.* **17**, 509 (2018).
- [12] A. M. Humphries, T. Wang, E. R. J. Edwards, S. R. Allen, J. M. Shaw, H. T. Nembach, J. Q. Xiao, T. J. Silva, and X. Fan, *Nat. Commun.* **8**, 911 (2017).
- [13] Note that an inverse spin-orbit filtering effect was predicted in [45]. In that work, a charge current flowing out of plane generates a pure spin current flowing in plane.
- [14] J. C. Slonczewski, *Phys. Rev. B* **39**, 6995 (1989).
- [15] J. Slonczewski, *J. Magn. Magn. Mater.* **159**, L1 (1996).
- [16] L. Berger, *Phys. Rev. B* **54**, 9353 (1996).
- [17] D. Ralph and M. Stiles, *J. Magn. Magn. Mater.* **320**, 1190 (2008).
- [18] M. D. Stiles and A. Zangwill, *Phys. Rev. B* **66**, 014407 (2002).
- [19] K. D. Belashchenko, A. A. Kovalev, and M. van Schilfhaarde, *Phys. Rev. Lett.* **117**, 207204 (2016).
- [20] K. Dolui and B. K. Nikolić, *Phys. Rev. B* **96**, 220403 (2017).
- [21] L. Wang, R. J. H. Wesselink, Y. Liu, Z. Yuan, K. Xia, and P. J. Kelly, *Phys. Rev. Lett.* **116**, 196602 (2016).
- [22] J. Zemen, J. Maek, J. Kuera, J. Mol, P. Motloch, and T. Jungwirth, *J. Magn. Magn. Mater.* **356**, 87 (2014).
- [23] We use a multiorbital tight binding model based on the Slater-Koster method [46], with parameters fitted to reproduce *ab initio* electronic structure calculations [47] including spin-dependent on site energies. We calculate the Fermi level by requiring charge neutrality of the layers. The spin-orbit coupling from [48] is used for all atoms. The hopping parameters at the interfaces are obtained as geometric averages of hopping parameters in neighboring atoms.
- [24] K. Xia, M. Zwierzycki, M. Talanana, P. J. Kelly, and G. E. W. Bauer, *Phys. Rev. B* **73**, 064420 (2006).
- [25] S. Wang, Y. Xu, and K. Xia, *Phys. Rev. B* **77**, 184430 (2008).
- [26] Without spin-orbit coupling, the spin torque on each principal layer is the difference between the spin currents at the boundaries of that principal layer. In the presence of spin-orbit coupling this relation does not hold due to coupling to the crystal lattice. To account for this, all spin torques are evaluated using the operator $J_{\text{ex}} \hat{\sigma} \times \hat{\mathbf{m}}$, where the exchange field J_{ex} is orbital dependent and determined by the Stoner splitting taken from first principles calculations of bulk metals found in [47].
- [27] W. Thomson, *Proc. R. Soc. A* **8**, 546 (1856).
- [28] T. McGuire and R. Potter, *IEEE Trans. Magn.* **11**, 1018 (1975).
- [29] C. Gould, C. Ruster, T. Jungwirth, E. Girgis, G. M. Schott, R. Giraud, K. Brunner, G. Schmidt, and L. W. Molenkamp, *Phys. Rev. Lett.* **93**, 117203 (2004).
- [30] A. N. Chantis, K. D. Belashchenko, E. Y. Tsybmal, and M. van Schilfhaarde, *Phys. Rev. Lett.* **98**, 046601 (2007).
- [31] N. Nagaosa, J. Sinova, S. Onoda, A. H. MacDonald, and N. P. Ong, *Rev. Mod. Phys.* **82**, 1539 (2010).
- [32] G. E. W. Bauer, E. Saitoh, and B. J. van Wees, *Nat. Mater.* **11**, 391 (2012).
- [33] V. P. Amin, J. Zemen, J. Železný, T. Jungwirth, and J. Sinova, *Phys. Rev. B* **90**, 140406 (2014).
- [34] C. López-Moníns, A. Matos-Abiague, and J. Fabian, *Phys. Rev. B* **90**, 174426 (2014).
- [35] E. Sagasta, Y. Omori, M. Isasa, M. Gradhand, L. E. Hueso, Y. Niimi, Y. C. Otani, and F. Casanova, *Phys. Rev. B* **94**, 060412 (2016).
- [36] T. Tanaka, H. Kontani, M. Naito, T. Naito, D. S. Hirashima, K. Yamada, and J. Inoue, *Phys. Rev. B* **77**, 165117 (2008).
- [37] J.-C. Rojas-Sánchez, N. Reyren, P. Laczkowski, W. Savero, J.-P. Attané, C. Deranlot, M. Jamet, J.-M. George, L. Vila, and H. Jaffrès, *Phys. Rev. Lett.* **112**, 106602 (2014).
- [38] M.-H. Nguyen, D. C. Ralph, and R. A. Buhrman, *Phys. Rev. Lett.* **116**, 126601 (2016).
- [39] J. D. Gibbons, D. MacNeill, R. A. Buhrman, and D. C. Ralph, *Phys. Rev. Applied* **9**, 064033 (2018).
- [40] A. Bose, D. D. Lam, S. Bhuktare, S. Dutta, H. Singh, Y. Jibiki, M. Goto, S. Miwa, and A. A. Tulapurkar, *Phys. Rev. Applied* **9**, 064026 (2018).
- [41] K. S. Das, W. Y. Schoemaker, B. J. van Wees, and I. J. Vera-Marun, *Phys. Rev. B* **96**, 220408 (2017).
- [42] T. Taniguchi, J. Grollier, and M. D. Stiles, *Phys. Rev. Applied* **3**, 044001 (2015).

- [43] H. B. M. Saidaoui and A. Manchon, *Phys. Rev. Lett.* **117**, 036601 (2016).
- [44] M. B. Lifshits and M. I. Dyakonov, *Phys. Rev. Lett.* **103**, 186601 (2009).
- [45] J. Linder and T. Yokoyama, *Phys. Rev. Lett.* **106**, 237201 (2011).
- [46] J. C. Slater and G. F. Koster, *Phys. Rev.* **94**, 1498 (1954).
- [47] L. Shi and D. A. Papaconstantopoulos, *Phys. Rev. B* **70**, 205101 (2004).
- [48] L. Visscher and K. Dylla, *At. Data Nucl. Data Tables* **67**, 207 (1997).